Plant Physiology and Biochemistry 127 (2018) 88–96

Contents lists available at ScienceDirect

Plant Physiology and Biochemistry

journal homepage: www.elsevier.com/locate/plaphy

Research article

The phytochelatin synthase from *Nitella mucronata* (Charophyta) plays a role in the homeostatic control of iron(II)/(III)

Debora Fontanini[a], Andrea Andreucci[a], Monica Ruffini Castiglione[a], Adriana Basile[b], Sergio Sorbo[c], Alessandro Petraglia[d], Francesca Degola[d], Erika Bellini[a,e], Laura Bruno[e], Claudio Varotto[f], Luigi Sanità di Toppi[a,*]

[a] Department of Biology, University of Pisa, Pisa, Italy
[b] Department of Biology, University of Naples "Federico II", Naples, Italy
[c] CeSMA, Microscopy Section, University of Naples "Federico II", Naples, Italy
[d] Department of Chemistry, Life Sciences and Environmental Sustainability, University of Parma, Parma, Italy
[e] Department of Biology, University of Rome "Tor Vergata", Rome, Italy
[f] Department of Biodiversity and Molecular Ecology, "Edmund Mach" Foundation, S. Michele all'Adige (TN), Italy

ARTICLE INFO

Keywords:
Cadmium
Charophytes
Iron
Metals
Phytochelatins
Phytochelatin synthase

ABSTRACT

Although some charophytes (*sister* group to land plants) have been shown to synthesize phytochelatins (PCs) in response to cadmium (Cd), the functional characterization of their phytochelatin synthase (PCS) is still completely lacking. To investigate the metal response and the presence of PCS in charophytes, we focused on the species *Nitella mucronata*. A 40 kDa immunoreactive PCS band was revealed in mono-dimensional western blot by using a polyclonal antibody against *Arabidopsis thaliana* PCS1. In two-dimensional western blot, the putative PCS showed various spots with acidic isoelectric points, presumably originated by post-translational modifications. Given the PCS constitutive expression in *N. mucronata*, we tested its possible involvement in the homeostasis of metallic micronutrients, using physiological concentrations of iron (Fe) and zinc (Zn), and verified its role in the detoxification of a non-essential metal, such as Cd. Neither *in vivo* nor *in vitro* exposure to Zn resulted in PCS activation and PC significant biosynthesis, while Fe(II)/(III) and Cd were able to activate the PCS *in vitro*, as well as to induce PC accumulation *in vivo*. While Cd toxicity was evident from electron microscopy observations, the normal morphology of cells and organelles following Fe treatments was preserved. The overall results support a function of PCS and PCs in managing Fe homeostasis in the carophyte *N. mucronata*.

1. Introduction

On the basis of their chemical properties, a number of heavy metals have been selected during plant evolution, becoming essential to several processes. The most important [i.e., iron (Fe), zinc (Zn), copper (Cu), and manganese (Mn)] are cofactors often required for enzyme activities and transcriptional regulation (Marschner, 2012). However, although being essential up to certain levels, these elements may become toxic at supraoptimal concentrations. Similarly, toxic effects can be exerted by submicro-to micromolar concentrations of non-essential metal(loid)s, such as cadmium (Cd), lead (Pb), mercury (Hg), arsenic (As), etc. (Rea et al., 2004).

Since plants acquire essential elements from their surroundings, they need an efficient system to obtain and maintain physiological levels of the required ions and, simultaneously, to quickly discriminate between essential and non-essential ones. A widespread strategy evolved by plants to regulate intracellular levels of heavy metals operates through phytochelatins (PCs), a class of heavy metal-inducible, cysteine-rich oligopeptides that segregate metal ions, particularly Cd, in vacuolar/lysosomal compartments (Cobbett and Goldsbrough, 2002). PCs are produced by the enzyme phytochelatin synthase (PCS; EC 2.3.2.15), a γ-glutamylcysteine dipeptidyl (trans)-peptidase, constitutively expressed in the cytosol and belonging to the clan CA of papain-like cysteine proteases (Vivares et al., 2005; Romanyuk et al., 2006; Rea, 2012).

In stark contrast to the significant number of studies carried out on the PCS function in angiosperms, only a few investigations have been performed on early plant lineages, despite their importance as fundamental landmarks in evolution. Charophytes (Charophyta; *syn.*, basal Streptophyta) are a paraphyletic group of green algae sharing several

Abbreviations: ESI-MS, electrospray ionization mass-spectrometry; GSH, reduced glutathione; MS/MS, tandem mass spectrometry; PC, phytochelatin; PCS, phytochelatin synthase

* Corresponding author. Department of Biology, via Luca Ghini, 13, 56126 Pisa, Italy.
E-mail address: luigi.sanita@unipi.it (L. Sanità di Toppi).

https://doi.org/10.1016/j.plaphy.2018.03.014
Received 9 February 2018; Received in revised form 10 March 2018; Accepted 12 March 2018
Available online 13 March 2018
0981-9428/

strong biochemical, molecular, physiological, and ultrastructural similarities with land plants (Leliaert et al., 2012; Domozych et al., 2016; Harholt et al., 2016; Holzinger and Pichrtová, 2016). As charophytes encompass the putative algal ancestor of land plants (Hori et al., 1985; Kenrick and Crane, 1997; McCourt et al., 2004; Qiu et al., 2006; Qiu, 2008; Becker and Marin, 2009; Wodniok et al., 2011; Leliaert et al., 2012; Bowman, 2013; Wickett et al., 2014; Delwiche and Cooper, 2015; Domozych et al., 2016; Harholtet al., 2016; Holzinger and Pichrtová, 2016), they can provide important "primeval" information, which is fundamental in reconstructing several biological functions from an evolutionary point of view (Schneider et al., 2015; Domozych et al., 2016; Lütz-Meindl, 2016). In this regard, it has been hypothesized that, from the Ordovician-Silurian periods onwards (or even before, beginning from the middle Cambrian; Graham et al., 2014; Morris et al., 2018), a number of charophytes moved from water environments to limnetic transition areas, and then to land environments, where they were presumably exposed to novel or more severe levels of stress, e.g., drought, extreme temperatures, UV radiation, etc. (Graham, 1996; Becker and Marin, 2009; Graham et al., 2014). Even more so, some terrestrial charophytes competed successfully with early land plants in the course of the Ordovician (Graham et al., 2014).

As far as PC synthesis in extant charophytes is concerned, Volland et al. (2013) showed that, under Cd treatment, the unicellular *Micrasterias denticulata* (Zygnematales) produced PCs. Furthermore, although Petraglia et al. (2014) did not detect any immunoreactive PCS signal in *Spirogyra* sp. (Zygnematales), *Chara vulgaris* (Charales) and *Coleochaete scutata* (Coleochaetales), they demonstrated that these charophytes were able to synthesize Cd-induced PCs, in particular the oligopeptides PC_2, PC_3 and PC_4.

Besides the well-known role of PCs in non-essential metal(loid)-detoxification (Cobbett and Goldsbrough, 2002), these thiol-peptides may also play a part in the regulation of essential metal homeostasis, as preliminarily demonstrated in angiosperms (Grill et al., 1988; Loscos et al., 2006; Ramos et al., 2008; Tennstedt et al., 2009; Vurro et al., 2011). The main objection to an exclusive role of PCs in plant cell detoxification of non-essential metal(loid)s is based on various characteristics of the PCS enzyme, namely: i) its constitutive expression, independent on exposition to toxic metal(loid)s (Clemens and Peršoh, 2009); ii) the apparently ubiquitous presence of homologous PCS gene (s) in plants growing in ecosystems that are geographically distant from heavy metal contamination (Clemens, 2006; Clemens and Peršoh, 2009; Volland et al., 2013; Olsson et al., 2017); iii) the recurrent absence of a correlation between PC levels and adaptive metal tolerance, the latter being typical of metal-hyperaccumulating plants, which are able to accumulate extremely high concentrations of metals without relying on a "hyper-enhanced" synthesis of PCs (Rascio and Navari-Izzo, 2011).

The possible involvement of PCS in the homeostatic control of metal micronutrients, such as Fe(II)/(III) and Zn, however, is still unclear in almost all land plants, as well as in charophytes. Actually, although Fe has always been abundant in the Earth's crust, it has had and continues to have serious bioavailability and insolubility problems, particularly in the aqueous medium (Cox, 1995; Fraústo da Silva and Williams, 2001), and specifically in freshwaters, in which most extant charophytes commonly live. Fe also possesses borderline chemical/environmental properties, in that it can potentially bind various atoms, including the sulphur (S) (Cox, 1995) of the thiolic groups of PCs. Thus, Fe can reasonably become a substrate for PCS, as it has been shown in the ancient liverwort *Lunularia cruciata*, where Fe(II) (and, slightly, Zn) activated the PCS enzyme *in vitro* (Degola et al., 2014).

When delving into the past to understand the present, it is extremely important to focus on organisms that can provide primeval information. The charophyte genus *Nitella* is considered to be a close algal relative of land plants (Hori et al., 1985; Graham, 1996; McCourt et al., 2004; Qiu, 2008), and from an ecological point of view it usually inhabits freshwater environments with intermediate trophic levels (Caisová et al., 2008) where metal micronutrients often represents growth-limiting factors (Urbaniak and Gąbka, 2014). Therefore, a possible role of PCs as fine regulators of physiological needs of Fe and other metal micronutrients would appear to be important in the case. In this work, the species *N. mucronata* was hence chosen as a model plant to verify: (a) if the PCS enzyme is constitutively expressed in charophytes; and (b) if the induced PCs may play a role not only in Cd detoxification, but also in the homeostatic control of Fe(II)/(III) and Zn needs.

2. Materials and methods

2.1. Plant material and growth conditions

Samples of *Nitella mucronata* (A.Braun) F.Miquel (common name "compact stonewort"; Charophyta) were collected from freshwater springs located in Parma surroundings (Italy) in April–May 2014/15/16. The material was immediately rinsed with double-distilled water, carefully checked under a stereo-microscope (WILD, Heerbrugg, Switzerland) and under an Olympus BH2 microscope 40X (Olympus Italia, Segrate, Italy) for the absence of potential biological contaminants (i.e., *Cyanobacteria*, *Chlorophyta*, etc.), and then cultivated as a monoculture in a growth chamber in the conditions detailed below.

Each sample, made up by a central stalk and some whorls of radiating branches (without the presence of reproductive structures, i.e., antheridia, oogonia, etc.), was transferred into a sterilized culture tube (Falcon™ 15 mL), filled with 12 mL of commercial oligomineral water, having the following ion composition (μM): NO_3^- 16.1, Ca^{2+} 284.4, Mg^{2+} 189.3, Na^+ 435.0, K^+ 7.7, SO_4^{2-} 321.7, Cl^- 104.4, $Cu^{tot} < 1.6$, $Fe^{tot} < 0.2$, $Al^{3+} < 0.37$, $Zn^{2+} < 0.01$, pH 6.7 at 20 °C.

The culture tubes were divided in groups, in which the following metal concentrations were added ($n = 5$ for each concentration/each valence): 7.5–30 μM Fe(II) ($FeSO_4$), or 7.5–30 μM Fe(III) [$Fe_2(SO_4)_3$], or 18–36 μM Cd ($CdSO_4$), or 30 μM Zn ($ZnSO_4$). The metal concentrations chosen for the experiments were based on preliminary tests (L. Sanità di Toppi, unpublished data) and on Chiaudani and Vighi (1977), Marschner (2012), Immers et al. (2013), Degola et al. (2014), and Petraglia et al. (2014). In the same number of culture tubes, no metals were added (controls), but supplied with an identical volume of the above oligomineral water, as for metal treatments. All tubes were placed in a growth chamber at 20 ± 1 °C for 5 days, under a photoperiod of 16 h light (PPFD = 60 μmol m^{-2} s^{-1})/8 h dark.

After rinsing with double-distilled water, the samples were gently blotted dry with filter paper, individually placed in other sterilized tubes (Falcon™ 15 mL), frozen in liquid nitrogen, and briefly stored at −80 °C for further analyses.

2.2. Mono-dimensional- and two-dimensional western blotting of phytochelatin synthase

Proteins from *N. mucronata* samples (central stalk and branches from three biological replicates, 200 mg FW each), untreated with metals (controls), were extracted with 400 μL lysis buffer, as described in Petraglia et al. (2014). The total protein content was determined according to the Bradford protein assay (Bradford, 1976), using bovine serum albumin as standard. For mono-dimensional (1-D) electrophoresis, 18 μg of total protein per well were loaded on a 12% SDS-polyacrylamide gel and electro-transferred at 100 V for 60 min onto a nitrocellulose membrane (GE Healthcare Bio-Sciences AB, Uppsala, Sweden) using the Mini Trans-Blot cell apparatus (Bio-Rad Laboratories, CA, USA). Protein loading and transfer efficiency of extracts were verified by the Ponceau-S staining (not shown). For two-dimensional (2-D) electrophoresis, protein extracts were precipitated with trichloroacetic acid/acetone, then re-suspended in a rehydration buffer (8 M urea, 2% w/v CHAPS, 50 mM DTT, 0.2% v/v Bio-Lyte 3/10 Bio-Rad ampholites, Bromophenol Blue in traces), and 125 μg of proteins were loaded on 7 cm-long ReadyStrip®IPG Strips, pH interval 3.0–10.0. 2D-electrophoresis was carried out using the Protean IEF system (Bio-

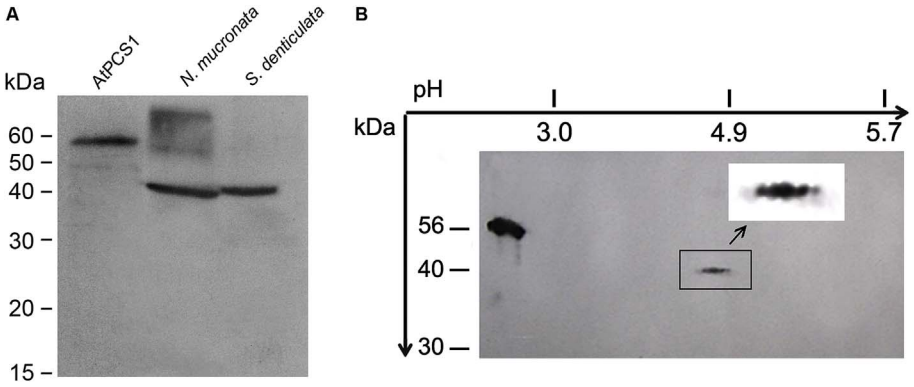

Fig. 1. Immunochemical characterization of *N. mucronata* putative phytochelatin synthase (PCS). (A) 1-D western blot of *N. mucronata* total protein extract (metal-untreated), showing an immunoreactive PCS band of about 40 kDa, compared with the putative PCS (40 kDa) from *Selaginella denticulata* (lycophyte) and the recombinant AtPCS1 (56 kDa) from *Arabidopsis thaliana*. **(B)** 2-D western blot of *N. mucronata* total protein extract, with a multispot PCS signal of about 40 kDa, pI 4.8–4.9 (framed by the rectangle); on the left, the recombinant AtPCS1 (56 kDa) run on the second dimension only. The inset shows a magnification of the five-spot-signal given by the putative PCS from *N. mucronata*. For both immunochemical analyses, a polyclonal antibody raised against *A. thaliana* PCS1 was employed. Both 1-D and 2-D western blots were performed in triplicate, and representative ones are shown in the figure.

Rad), following the manufacturer's instruction. Gels were then stained with SYPRO® Ruby Protein Stain (Bio-Rad) and images acquired using the Versadoc Imaging System (Bio-Rad). After the image digitization, gels were immersed for 20 min in Laemmli buffer (Laemmli, 1970) and briefly washed with transfer buffer (25 mM Tris, 192 mM glycine, pH 8.3, 20% v/v methanol), then proteins were electro-transferred on nitrocellulose membrane as described above.

For both 1-D and 2-D western blot analyses, immunoreactivity was assayed with a polyclonal antibody (diluted 1:5000 in blocking buffer and probed for 2 h) raised against *A. thaliana* PCS1 (AtPCS1, 56 kDa) (Ruotolo et al., 2004). The membranes were incubated with a secondary antibody (anti-rabbit linked to peroxidase activity for ECL, Amersham, GE Healthcare), at a dilution of 1:5000, for 1 h. The peroxidase activity was developed by ECL solutions (ECL western-blot Detection, Amersham, GE Healthcare).

2.3. Phytochelatin synthase activity assays and phytochelatin characterization by HPLC-mass spectrometry

N. mucronata PCS activity was assayed in central stalk and branches (250 mg FW per sample), cut from plants cultivated as described above, in the absence of any supplied metal (control). All the material was assayed *in vitro*, mainly following the protocol by Wojas et al. (2008) and Petraglia et al. (2014), with the only difference that, for each metal to be tested, the extraction and reaction buffers contained (one at a time): 50 µM Fe(II), 100 µM Fe(II), 30 µM Fe(III), 50 µM Fe(III), 100 µM Fe(III), 100 µM Cd, 30 µM Zn, 50 µM Zn (salt forms as in point 2.1), and the same volume of double-distilled water in controls. After an incubation-time of 90 min at 35 °C, and termination of the reaction with 125 µL 20% trichloroacetic acid, the measure of the PCS activity was immediately performed by HPLC-electrospray ionization mass-spectrometry (HPLC-ESI-MS) with a LTQ Orbitrap XL (ThermoElectron Corporation, MA, USA), set as described in Petraglia et al. (2014). Chromatographic elution was carried out on a Supelco Ascentis Express r. p. C_{18} column (Sigma-Aldrich, Milan, Italy). The PCS *in vitro* activity was determined from the integrated PC peak areas, and expressed as pmol PCs g^{-1} FW min^{-1}. For the *in vivo* detection of PCs, the metal-treated and control plants (250 mg FW for each sample, central stalk and branches) were homogenised in mortar, in ice-cold 5% (w/v) 5-sulfosalicylic acid containing 6.3 mM diethylenetriaminepentaacetic acid (DTPA), according to de Knecht et al. (1994) and Petraglia et al. (2014). After centrifugation at 10,000x*g* for 10 min at 4 °C, the supernatants were filtered through Minisart RC4 0.45 µm filters (Sartorius, Goettingen, Germany) and immediately assayed by HPLC-ESI-MS (followed by HPLC-ESI-MS/MS), as detailed in Petraglia et al. (2014).

2.4. Transmission electron microscopy and X-ray microanalysis

For transmission electron microscopy (TEM), 5-mm segments from fresh *N. Mucronata* untreated branches (control), or exposed to 30 µM Fe(II), or 30 µM Fe(III), or 30 µM Zn, or 36 µM Cd, were fixed at room temperature for 2 h in 3% glutaraldehyde dissolved in 0.065 M phosphate buffer, pH 7.2–7.4, postfixed for 1.5 h at room temperature with 1% OsO_4 in the same buffer, dehydrated with ethanol up to propylene oxide, and finally embedded in Spurr's epoxy resin for 24 h at 70 °C. At least 30 ultrathin sections (40 nm-thick) were mounted on Cu grids, stained with Uranyl Replacement Stain UAR (Electron Microscopy Sciences, Hatfield, PA, USA), as described in Nakakoshi et al. (2011), and with Reynold's lead citrate, then observed by a Philips EM 208S TEM (Philips, Eindhoven, The Netherlands) at an accelerating voltage of 80 kV.

For TEM X-ray microanalysis, at least 30 unstained ultrathin sections (40 nm-thick) of branches, exposed to the same metals as above (plus controls), were fixed, postfixed, dehydrated and embedded in Spurr's epoxy resin (see above), mounted on 100-mesh nylon grids and placed in a Jeol JEM-2010 TEM (Jeol Italia S. p.A., Basiglio, MI, Italy), equipped with the energy dispersive X-ray spectrometer "Oxford INCA 100". The accelerating voltage was 20 kV and the specimen probe size 30–50 nm in diameter. X-ray counts were made on 30 different areas per sample, over a counting time of 100 s.

2.5. Statistics

Differences were evaluated by the nonparametric Kruskal-Wallis test ($p < 0.05$ and < 0.01), SPSS version 20.0 (IBM-SPSS Statistics, Armonk, NY, USA). Results were expressed as mean ± SE, $n = 5$. All the experiments were performed at least three times.

3. Results

3.1. Western blotting of phytochelatin synthase

In 1-D western blot analysis, *N. mucronata* showed a constitutive, western-immunoreactive PCS signal with a molecular mass of approx. 40 kDa (Fig. 1A). In 2-D western blot, an acidic constitutive PCS signal of about 40 kDa was detected (Fig. 1B). As highlighted by magnification (inset of Fig. 1B), the 2-D signal consisted of about five immunoreactive spots. The metals inducing the PCS activity *in vitro* were Fe(III) ≥ Cd = Fe(II), whereas Zn did not affect such activity, compared with controls (Table 1A). Fe(II) and Cd induced the *in vitro* synthesis of PC_2 only, whereas Fe(III) induced the synthesis of PC_3 as well.

3.2. Phytochelatin synthase activity and phytochelatin characterization upon metal ion treatments

The ability of *N. mucronata* to synthesize PCs *in vivo* was verified after a 5-day-exposure to different metals (and relative controls). The results, presented in Table 1B, showed that the PCS was activated by Fe (III) = Cd ≥ Fe(II), thus substantially confirming the overall results of the *in vitro* assays (Table 1A). In particular, 18 µM Cd induced *in vivo*

Table 1A
***In vitro* activity of phytochelatin synthase (PCS) detected in extracts from *N. mucronata* plants**, incubated for 90 min at 35 °C in the proper reaction mixture (details in 2.3), in the presence or absence (control) of the metal concentrations indicated below. ($n = 5$; mean ± SE. Different letters indicate significant differences at $p < 0.05$).

	PCS activity (pmol PCs g^{-1} FW min^{-1})
Fe(II) 50 μM	85.7 ± 11.4 a
Fe(II) 100 μM	168.3 ± 57.9 a
Fe(III) 30 μM	276.1 ± 29.2 b
Fe(III) 50 μM	291.9 ± 12.7 b
Fe(III) 100 μM	167.1 ± 25.4 a
Cd 100 μM	141.3 ± 35.5 a
Zn 30 μM	n.d.
Zn 50 μM	n.d.
Control	n.d.

(n.d. = not detected).
NB: Fe(II) and Cd induced the *in vitro* synthesis of PC_2 only, whereas Fe(III) induced both PC_2 and PC_3.

Table 1B
Levels of phytochelatins (PC_2, PC_3, PC_4, and total PCs) in *N. mucronata* plants exposed for 5 days to the metal concentrations indicated below. ($n = 5$; mean ± SE. Different letters indicate significant differences at $p < 0.05$).

	PC_2	PC_3	PC_4	Total PCs
	(nmol PC g^{-1} FW)			
Fe(II) 7.5 μM	18.5 ± 1.3	n.d.	n.d.	18.5 ± 1.3 a
Fe(II) 30 μM	12.7 ± 1.6	n.d.	n.d.	12.7 ± 1.6 b
Fe(III) 7.5 μM	19.6 ± 1.0	n.d.	n.d.	19.6 ± 1.0 a
Fe(III) 30 μM	40.1 ± 6.2	n.d.	n.d.	40.1 ± 6.2 c
Cd 18 μM	11.8 ± 2.4	9.4 ± 1.9	1.4 ± 0.2	22.6 ± 4.5 ad
Cd 36 μM	17.5 ± 6.7	16.3 ± 2.3	n.d.	33.8 ± 9.0 acd
Zn 30 μM	7.1 ± 3.7	n.d.	n.d.	7.1 ± 3.7 be
Control	5.5 ± 2.4	n.d.	n.d.	5.5 ± 2.4 e

(n.d. = not detected).

synthesis of PC_2, PC_3 and traces of PC_4, 36 μM Cd induced PC_2 and PC_3, but not PC_4, whereas Fe(II)/(III) induced the production of PC_2 only, the strongest response being observed with 30 μM Fe(III), the lowest with 30 μM Fe(II), and intermediate with 7.5 μM Fe(II)/(III) (Table 1B). In Zn-exposed plants, almost undetectable levels of PC_2 were measured, as to the controls (Table 1B). Fig. 2A shows representative HPLC-ESI-MS chromatograms of the PCs produced by *N. mucronata*, exposed to 18 μM Cd for 5 days. The chromatograms for Fe(II)/(III)-induced PCs *in vivo* were nearly identical, except for the lack of PC_3 and PC_4. PC_2 and PC_3 identities were confirmed by the relative MS/MS fragmentation patterns (Fig. 2B).

3.3. Ultrastructural analyses

Branches of *N. mucronata* samples not exposed to the metals (control) showed a normal ultrastructure (Fig. 3A–C). The cells, surrounded by thick walls, contained ovoidal chloroplasts with a well-developed thylakoid system and abundant starch. The mitochondria showed numerous cristae and an electron dense matrix. By contrast, Cd-exposed samples were severely damaged; the starch deposits almost completely disappeared, the thylakoid system was disarrayed (Fig. 3D–E), and the cytoplasm contained multilamellar/multivesicular bodies (Fig. 3F). In both Fe(II) and Fe(III)-exposed samples, the chloroplasts retained instead a normal ultrastructure and abundant starch (Fig. 3G, H, J), and mitochondria showed a well-preserved appearance (Fig. 3I, L). A prominent feature of Fe(III)-exposed samples was the presence of cytoplasmic vesicles with an electron dense content (Fig. 3K); X-ray microanalysis showed a Fe peak associated with these structures (see Fig. 3P for a representative spectrum). Finally, Zn-exposed samples showed cells with a normal and well-conserved ultrastructure (Fig. 3M–O).

4. Discussion

The discovery of the ability to produce PCs even in very ancient plant lineages, following a rapid activation of constitutive PCSs (Degola et al., 2014; Petraglia et al., 2014), poses the fundamental question whether PCs and PCSs should be exclusively considered as part of a mere non-essential metal(loid)-detoxifying mechanism, or as components of a broader system aimed at regulating essential metal homeostasis. With the aim to provide a more comprehensive picture in this direction from a phylogenetic point of view, we verified whether PCS is constitutively expressed and active in *N. mucronata*, a member of charophytes, soundly demonstrated to be close relatives (*sister* group) of land plants (see the relative refs. in the Introduction section). *N. mucronata* can in fact be investigated to assess whether primeval plants in past environmental conditions may have developed a metal ion-homeostasis regulating-system, which has been conserved up to the present days and further improved by land plants to adapt to the terrestrial environment.

In this work, a PCS enzyme was identified and immunocharacterized for the first time in a charophyte (specifically in *N. mucronata*), and tested against homeostatic concentrations of the essential metal micronutrients Fe(II)/(III) and Zn, as well as against the non-essential heavy metal Cd. The results of 1-D and 2-D western blots confirmed that *N. mucronata* constitutively expresses a putative PCS of about 40 kDa, which shows an almost identical molecular mass as the one from the lycophyte *Selaginella denticulata* (Petraglia et al., 2014). In this context, the *N. mucronata* PCS's molecular mass, compared to the much lighter/shorter PCSs of freshwater, non-extremophilic chlorophytes (i.e. *Chlamydomonas reinhardtii*, *Volvox carteri*, *Chlorella variabilis*, etc.; https://www.ncbi.nlm.nih.gov/protein/), could be seen as a "key-innovation" releasing old lineages from constraints, and enabling them to invade new adaptive environments (Graham, 1996). Actually, it has been suggested that increases in PCS mass/length may confer both a better thermal stability and a significant improvement in supporting broader responses to metal ions (Ruotolo et al., 2004), as well as in protecting the cells against metal-induced oxidative damage (Matsumoto et al., 2009). In fact, charophytes lived for very long time on lands – and were therefore well-adapted – before the full spread of land plants (Graham et al., 2014; Harholt et al., 2016). Some of them have returned back to freshwater environments after quite a long colonization of aeroterrestrial paleoenvironments, thus acquiring most of the biochemical-molecular and ultrastructural features typical of a number of early land plants, i.e. lycophytes as *S. denticulata* (Qiu et al., 2006; Delwiche and Cooper, 2015). Furtherly supporting this view, in the recently sequenced genome of the charophyte *Klebsormidium flaccidum* (Klebsormidiales), a putative PCS with a comparable length to that of land plants was identified (Hori et al., 2014). Unfortunately, previous attempts to immunochemically detect PCS bands in other charophytes, such as *Spirogyra* sp., *Chara vulgaris*, and *Coloechaete scutata*, failed, although all of them were able to produce significant amounts of Cd-induced PCs (Petraglia et al., 2014).

As far as the 2-D western blot of the *N. mucronata* PCS is concerned, it clearly shows a "train" of spots, suggesting the presence of multiple isoforms of the protein. This pattern could be due to increasing numbers of post-translational modifications, such as phosphorylation, which may result in protein isoelectric point shifts. In the case of AtPCS1, for which the constitutive expression has been shown at both transcriptional and translational levels (Cobbett, 2000; Vatamaniuk et al., 2000), post-translational modifications can be invoked as a means of regulating the enzyme activity. Wang et al. (2009) showed that the AtPCS1 can be post-translationally activated by a specific phosphorylation at the threonine 49 level, which is in close proximity to the catalytic site of PCS.

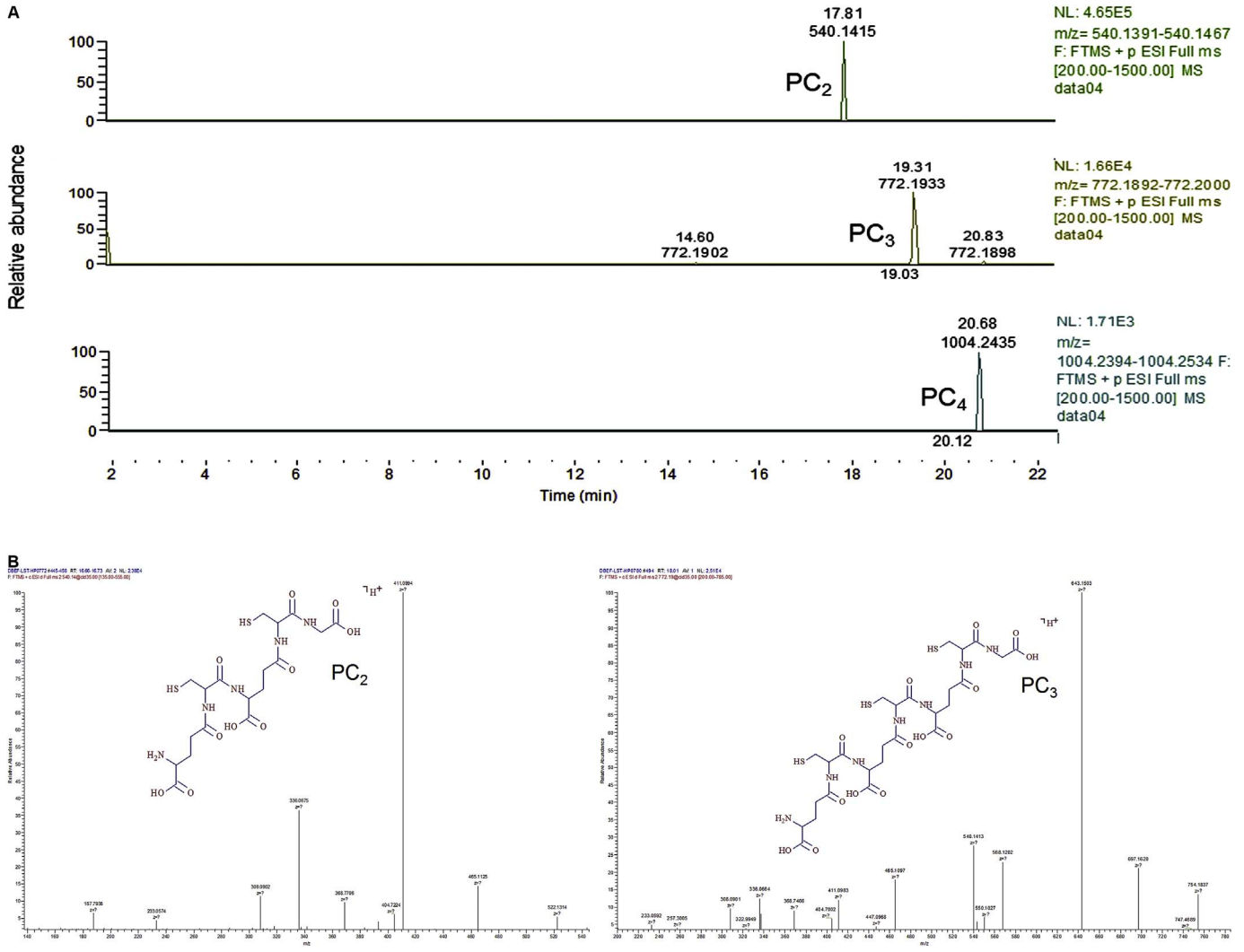

Fig. 2. Representative mass chromatograms and spectra of phytochelatins produced by *N. mucronata* exposed to 18 μM Cd for 5 days. (A) From the top to the bottom: PC_2, PC_3 and PC_4, with ESI-MS retention time and *m/z* indicated above the respective peak. The ESI-MS chromatogram given by 30 μM Fe(III) was identical to this one, except for PC_3 and PC_4 which were not induced *in vivo* (and PC_3 only *in vitro*). (NB: the two almost undetectable peaks preceding and following PC_3 are non-specific and do not represent signals for the thiol-peptide characterization). **(B)** Representative MS/MS fragmentation patterns for PC_2 (*m/z* 540.14) and PC_3 (*m/z* 772.19), and relative deduced formulae, at a normalized collision energy of 35 arbitrary units. For PC_4 (*m/z* 1004.24), the detected amounts were not sufficient for obtaining the MS/MS fragmentation patterns.

In spite of the evident difference in molecular mass between the putative *N. mucronata* PCS and the AtPCS1, the apparent conservation in immunological responsiveness suggests a possible mutual sequence resemblance, further evident in the *S. denticulata* PCS, which also possesses an almost identical molecular mass of that of *N. mucronata*.

From a functional point of view, the metal induction profile of *N. mucronata* PCS displays some good similarities with the PCSs of land plants. In fact, in modern tracheophytes, particularly in angiosperms, it has been observed that Fe was able to activate the PCS enzyme, thus leading to the conclusion that the synthesis of PCs might not only reflect a metal detoxification strategy, but also supports a PC involvement in the homeostasis of metal micronutrients, particularly Fe and Zn (Loscos et al., 2006; Ramos et al., 2008). Also the constitutively expressed PCS of the holoparasitic angiosperm *Cuscuta campestris*, and the associated PC production, were aimed at regulating the homeostasis of essential metals, such as Zn and Cu (Vurro et al., 2011). Moreover, Fe deficiency promoted the expression of PCS genes in *Vigna radiata* (Muneer et al., 2014) and increased the synthesis of Cd-induced PCs in *Hordeum vulgare* (Astolfi et al., 2012).

Detectable PC synthesis in *N. mucronata* is induced by relatively low concentrations of Fe, which, according to the ultrastructural analyses carried out, is not toxic for the plant. Overall, it appears reasonable that the induction of PCs by Fe could be triggered by the need to preserve homeostatic levels of the nutrient, rather than to control potentially toxic cellular concentrations. Thus, it is likely that at the relatively low Fe concentrations used in this study, PCs provided a prompt system for short-term control of Fe availability through its reversible accumulation in the vacuole and/or in vesicular bodies, in a process closely resembling the one employed by land plants for heavy metal detoxification (Peng and Gong, 2014). Also in the charophyte *M. denticulata*, exposure to Fe not only prevented ultrastructural alterations, but even improved cell development and photosynthetic activity under subsequent Cd exposure (Volland et al., 2014).

In our experiments, the extensive toxicity symptoms observed in *N. mucronata* exposed to 36 μM Cd (severely damaged chloroplasts, cytosolic multilamellar bodies, etc.), support the lack of efficient detoxification mechanisms, at least when Cd is supplied at this concentration. In addition, the lack of starch may suggest impairment of the photosynthetic activity. Similarly, chloroplast heavy alterations, the presence of multivesicular bodies, and autophagosome formation have been reported at Cd concentrations ranging from 5 to 150 μM in *M. denticulata* (Andosch et al., 2012; Volland et al., 2014), in the freshwater moss *Leptodictyum riparium* (Esposito et al., 2012) and in other bryophytes (Carginale et al., 2004; Basile et al., 2012, 2013; Degola et al., 2014).

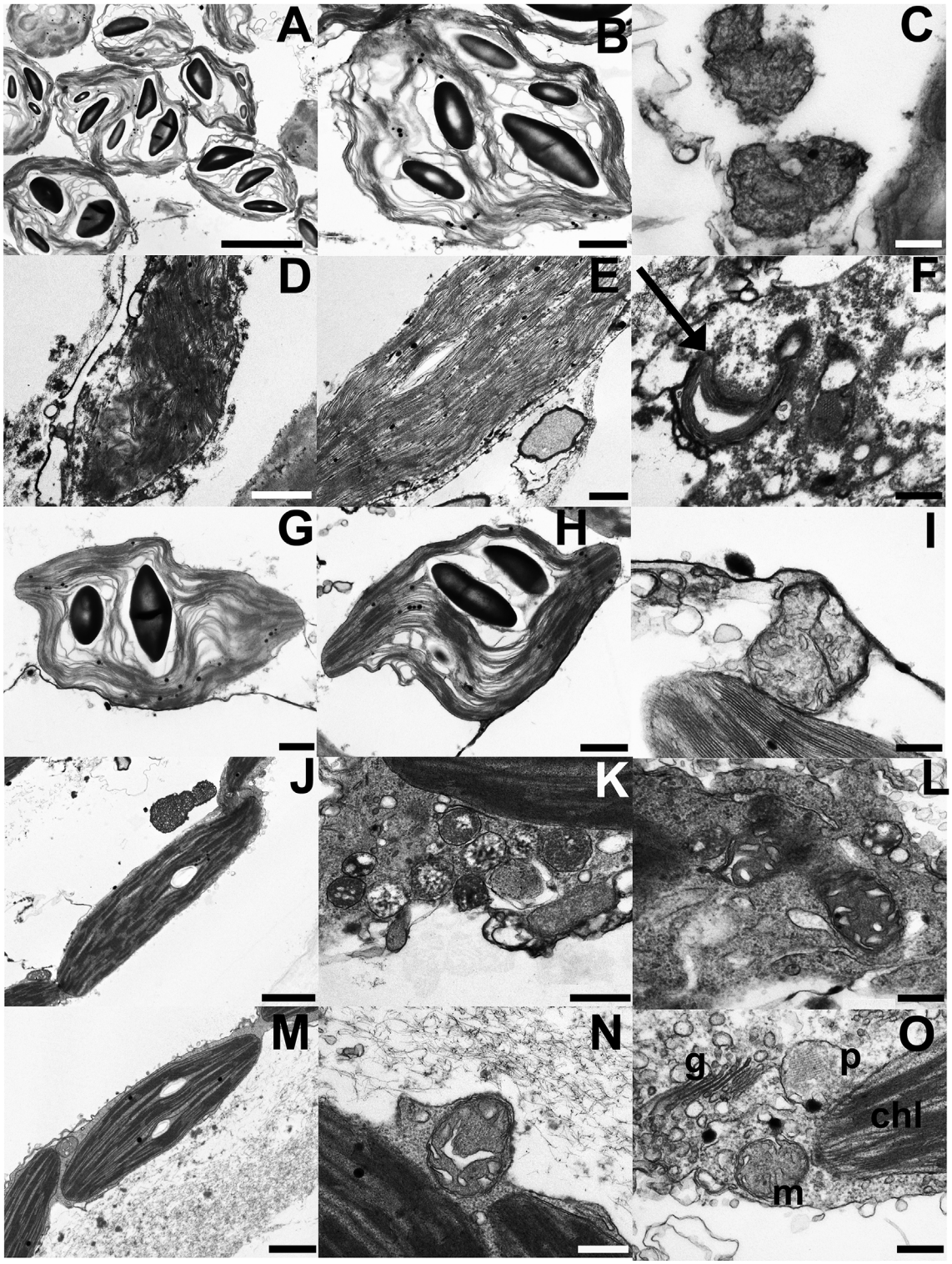

Fig. 3. TEM micrographs of ultrathin sections from branches of *N. mucronata*, non-exposed (A–C), or exposed to 36 μM Cd (D–F), 30 μM Fe(II) (G–I), 30 μM Fe(III) (J–L), 30 μM Zn (M–O). (A, B) Chloroplasts with normally developed thylakoids and starch grains. **(C)** Well-conformed mitochondria with an electron dense matrix. **(D)** A severely damaged chloroplast in Cd-exposed samples. The organelle appears misshapen and with a disorganized thylakoid system. **(E)** At a higher magnification, the chloroplast shows densely-packed thylakoids, although still arranged in grana and intergrana membranes. **(F)** A multilamellar body in the cytoplasm (arrow). **(G, H)** A chloroplasts with starch grains in Fe(II)-exposed samples. The thylakoid system is well-conformed and possesses organized grana and intergrana membranes. **(I)** Adherent to the chloroplast, a dividing mitochondrion with well-preserved cristae. (**J**) A chloroplast from Fe(III)-exposed samples with a starch grain and packed thylakoids, where grana and intergrana membranes are well-conformed. (**K**) A group of cytoplasmic vesicles with electron dense content, on which the X-ray microanalysis was performed (see the spectrum, **P**). (**L**) Mitochondria with well-conformed cristae and normal appearance. (**M**) A chloroplast with packed thylakoids in Zn-exposed samples. Grana and intergrana membranes and a starch grain are clearly visible. (**N**) A mitochondrion with some evident cristae. (**O**) Next to the mitochondrion (m), a well-preserved peroxisome (p) and a dictyosome (g). Scale bars: 5 μm (**A**); 2 μm (**B, J**); 1 μm (**D, G, H, M**); 500 nm (**E, K**); 300 nm (**C, F, I, L, N, O**). (**P**) Representative X-ray microanalysis spectrum, acquired inside the vesicles observed in Fig. 2**K** [Fe(III)-exposed samples], showing a main Fe peak (arrow) with Kα = 6.40 keV.

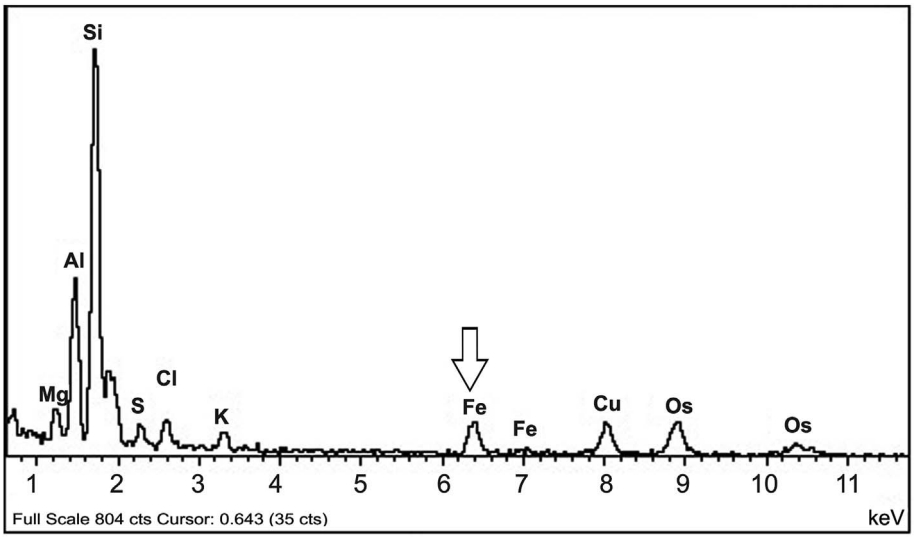

Fig. 3. (*continued*)

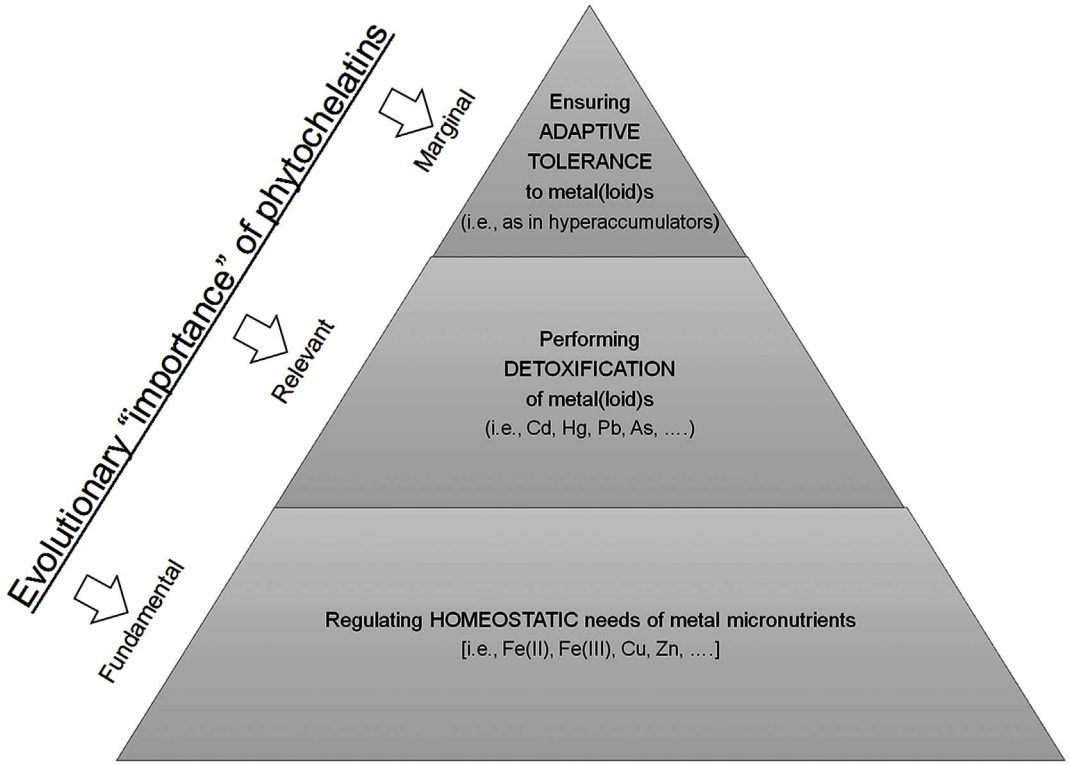

Fig. 4. Evolutionary importance of phytochelatins in metal(loid) homeostasis/detoxification/tolerance. Our general hypothesis, corroborated also by the data presented in this work, is that PCs are broadly necessary for controlling the homeostasis of metal micronutrients, particularly Fe(II)/(III). Besides, the high PC affinity towards a number of *sulphur-seeking* toxic metal(loid)s confers to these thiol-peptides the well-known ability to chelate and segregate them in the vacuolar/lysosomal compartment. However, as demonstrated by a number of experiments dealing with metal(loid)-hyperaccumulators, PCs are not responsible for the metal(loid) adaptive hypertolerance shown by these peculiar metallophytes. Thus, our hypothesis is that the evolutionary importance of PCs progressively decreases from the pyramid base (homeostatic needs) towards the middle part (detoxification), reaching the minimum at the top (adaptive tolerance).

Multilamellar/multivesicular bodies are ultrastructures often related to autophagy and endocytic phenomena (Thompson and Vierstra, 2005), and could originate as an accretion of undigested membranes from endocytosis. The appearance of autophagy after Cd treatment in *M. denticulata* could be regarded as a survival strategy aimed at eliminating severely damaged organelles (Andosch et al., 2012). Thus, these structures might perhaps contribute, together with PCs, to the intracellular defence against the toxic effects of Cd.

Finally, Zn treatments did not show any particular alteration in the *N. mucronata* cell ultrastructure, compared with controls. The substantial unresponsiveness of *N. mucronata* PCS to Zn indicates that in the course of plant evolution the specificity of PCS activation by different metals has been subjected to notable variation, since some PCSs have been shown to be induced by Zn, albeit at moderate levels (Grill et al., 1988; Loscos et al., 2006; Ramos et al., 2008; Tennstedt et al., 2009; Vurro et al., 2011; Degola et al., 2014).

Taken together, the results obtained in this work indicate that the PCS enzyme of the charophyte *N. mucronata* manages Fe(II)/(III) homeostasis and, at the same time, is activated by Cd stress. Digging deeper into PCSs and PCs (Fig. 4) present in other phototrophs with a

long evolutionary history will hopefully contribute to further clarifying this complex scenario.

Author contributions

DF, EB and LSdT wrote the manuscript and performed the phytochelatin and phytochelatin synthase analyses. AP and LB collected the material and make ready the algal culture. AA and CV helped to perform the phytochelatin analysis and contributed to write the manuscript. FD performed the phytochelatin synthase western blotting. MRC, AB and SS conducted the microscopical analysis. DF and LSdT coordinated the data collection and reviewed the manuscript.

Conflicts of interest

All the authors declare that the research was conducted in the absence of any commercial or financial relationships that could be construed as a potential conflict of interest.

Acknowledgments

Particular thanks to Prof. Simone Ottonello (University of Parma, Italy) for the kind gift of the *Arabidopsis thaliana* PCS1 antibody. The technical assistance of Dr. Andrea Faccini (Centro Interdipartimentale Misure "G. Casnati", University of Parma, Italy) and Dr. Mauro Zapparoli (Centro Interdipartimentale Grandi Strumenti, University of Modena and Reggio Emilia, Italy) is gratefully acknowledged. This work was kindly supported by MIUR-PRIN 2015 funds (prot. 20158HTL58, PI Prof. Luigi Sanità di Toppi).

References

Andosch, A., Affenzeller, M.J., Lütz, C., Lütz-Meindl, U., 2012. A freshwater green alga under cadmium stress: ameliorating calcium effects on ultrastructure and photosynthesis in the unicellular model *Micrasterias*. J. Plant Physiol. 169, 1489–1500. http://dx.doi.org/10.1016/j.jplph.2012.06.002.

Astolfi, S., Zuchi, S., Neumann, G., Cesco, S., Sanità di Toppi, L., Pinton, R., 2012. Response of barley plants to Fe deficiency and Cd contamination as affected by S starvation. J. Exp. Bot. 63, 1241–1250. http://dx.doi.org/10.1093/jxb/err344.

Basile, A., Sorbo, S., Conte, B., Cardi, M., Esposito, S., 2013. Ultrastructural changes and heat shock proteins 70 induced by atmospheric pollution are similar to the effects observed under in vitro heavy metals stress in *Conocephalum conicum* (Marchantiales-Bryophyta). Environ. Pollut. 182, 209–216. http://dx.doi.org/10.1016/j.envpol.2013.07.014.

Basile, A., Sorbo, S., Pisani, T., Paoli, L., Munzi, S., Loppi, S., 2012. Bioaccumulation and ultrastructural effects of Cd, Cu, Pb and Zn in the moss *Scorpiurum circinatum* (Brid.) Fleisch. &Loeske. Environ. Pollut. 166, 208–211. http://dx.doi.org/10.1016/j.envpol.2012.03.018.

Becker, B., Marin, B., 2009. Streptophyte algae and the origin of embryophytes. Ann. Bot. 103, 999–1004. http://dx.doi.org/10.1093/aob/mcp044.

Bowman, J.L., 2013. Walkabout on the long branches of plant evolution. Curr. Opin. Plant Biol. 16, 70–77. http://dx.doi.org/10.1016/j.pbi.2012.10.001.

Bradford, M.M., 1976. A rapid and sensitive method for the quantitation of microgram quantities of protein utilizing the principle of protein-dye binding. Anal. Biochem. 72, 248–254. http://dx.doi.org/10.1016/0003-2697(76)90527-3.

Caisová, L., Husák, Š., Komárek, J., 2008. *Nitella mucronata* (Br.) Miquel (Charophyta) in the Czech Republic. Fottea 8, 105–107. http://dx.doi.org/10.5507/fot.2008.005.

Carginale, V., Sorbo, S., Capasso, C., Trinchella, F., Cafiero, G., Basile, A., 2004. Accumulation, localisation, and toxic effects of cadmium in the liverwort *Lunularia cruciata*. Protoplasma 223, 53–61. http://dx.doi.org/10.1007/s00709-003-0028-0.

Chiaudani, G., Vighi, M., 1977. Applicazione di un saggio algale standard per lo studio di fenomeni di tossicità. Nuovi Ann. Ig. Microbiol. 28, 145–163.

Clemens, S., 2006. Evolution and function of phytochelatin synthases. J. Plant Physiol. 163, 319–332. http://dx.doi.org/10.1016/j.jplph.2005.11.010.

Clemens, S., Peršoh, D., 2009. Multi-tasking phytochelatin synthases. Plant Sci. 177, 266–271. http://dx.doi.org/10.1016/j.plantsci.2009.06.008.

Cobbett, C.S., 2000. Phytochelatins and their roles in heavy metal detoxification. Plant Physiol. 123, 825–832. http://dx.doi.org/10.1104/pp.123.3.825.

Cobbett, C., Goldsbrough, P., 2002. Phytochelatins and metallothioneins: roles in heavy metal detoxification and homeostasis. Annu. Rev. Plant Biol. 53, 159–182. http://dx.doi.org/10.1146/annurev.arplant.53.100301.135154.

Cox, P.A., 1995. The Elements on Earth: Inorganic Chemistry in the Environment. Oxford University Press, Oxford.

de Knecht, J.A., Van Dillen, M., Koevoets, P.L.M., Verkleij, J.A.C., Ernst, W.H.O., 1994. Phytochelatins in cadmium-sensitive and cadmium-tolerant *Silene vulgaris*. Chain length distribution and sulfide incorporation. Plant Physiol. 104, 255–261. http://dx.doi.org/10.1104/pp.104.1.255.

Degola, F., De Benedictis, M., Petraglia, A., Massimi, A., Fattorini, L., Sorbo, S., Basile, A., Sanità di Toppi, L., 2014. A Cd/Fe/Zn-responsive phytochelatin synthase is constitutively present in the ancient liverwort *Lunularia cruciata* (L.) Dumort. Plant Cell Physiol. 55, 1884–1891. http://dx.doi.org/10.1093/pcp/pcu117.

Delwiche, C.F., Cooper, E.D., 2015. The evolutionary origin of a terrestrial flora. Curr. Biol. 25, R899–R910. http://dx.doi.org/10.1016/j.cub.2015.08.029.

Domozych, D.S., Popper, Z.A., Sørensen, I., 2016. Charophytes: evolutionary giants and emerging model organisms. Front. Plant Sci. 10, 1470–1477. http://dx.doi.org/10.3389/fpls.2016.01470.

Esposito, S., Sorbo, S., Conte, B., Basile, A., 2012. Effects of heavy metals on ultrastructure and HSP70S induction in the aquatic moss *Leptodictyum riparium* Hedw. Int. J. Phytoremediation 14, 443–455. http://dx.doi.org/10.1080/15226514.2011.620904.

Fraústo da Silva, J.R., Williams, R.J.P., 2001. The Biological Chemistry of the Elements. The Inorganic Chemistry of Life, second ed. Oxford University Press, Oxford.

Graham, L.E., 1996. Green algae to land plants: an evolutionary transition. J. Plant Res. 109, 241–251. http://dx.doi.org/10.1007/BF02344471.

Graham, L.E., Lewis, L.A., Taylor, W., Wellman, C., Cook, M., 2014. Early terrestrialization: transition from algal to bryophyte grade. In: Hanson, D.T., Ricepp, S.K. (Eds.), Photosynthesis in Bryophytes and Early Land Plants. Springer, Dordrecht, pp. 9–28.

Grill, E., Thumann, J., Winnacker, E.-L., Zenk, M.H., 1988. Induction of heavy-metal binding phytochelatins by inoculation of cell cultures in standard media. Plant Cell Rep. 7, 375–378. http://dx.doi.org/10.1007/BF00269516.

Harholt, J., Moestrup, Ø., Ulvskov, P., 2016. Why plants were terrestrial from the beginning. Trends Plant Sci. 21, 96–101. http://dx.doi.org/10.1016/j.tplants.2015.11.010.

Holzinger, A., Pichrtová, M., 2016. Abiotic stress tolerance of charophyte green algae: new challenges for omics techniques. Front. Plant Sci. 7, 678–695. http://dx.doi.org/10.3389/fpls.2016.00678.

Hori, H., Lim, B.-L., Osawa, L., 1985. Evolution of green plants as deduced from 5S rRNA sequences. Proc. Natl. Acad. Sci. U.S.A. 82, 820–823.

Hori, K., Maruyama, F., Fujisawa, T., Togashi, T., Yamamoto, N., Seo, M., et al., 2014. *Klebsormidium flaccidum* genome reveals primary factors for plant terrestrial adaptation. Nat. Commun. 5, 3978. http://dx.doi.org/10.1038/ncomms4978.

Immers, A.K., Van der Sande, M.T., Van der Zande, R.M., Geurts, J.J.M., Van Donk, E., Bakker, E.S., 2013. Iron addition as a shallow lake restoration measure: impacts on charophyte growth. Hydrobiologia 710, 241–251. http://dx.doi.org/10.1007/s10750-011-0995-7.

Kenrick, P., Crane, P.R., 1997. The origin and early evolution of plants on land. Nature 389, 33–39. http://dx.doi.org/10.1038/37918.

Laemmli, U.K., 1970. Cleavage of structural proteins during the assembly of the head of Bacteriophage T4. Nature 227, 680–685. http://dx.doi.org/10.1038/227680a0.

Leliaert, F., Smith, D.R., Moreau, H., Herron, M.D., Verbruggen, H., Delwiche, C.F., De Clerck, O., 2012. Phylogeny and molecular evolution of the green algae. Crit. Rev. Plant Sci. 1, 1–46. http://dx.doi.org/10.1080/07352689.2011.615705.

Loscos, J., Naya, L., Ramos, J., Clemente, M.R., Matamoros, M.A., Becana, M., 2006. A reassessment of substrate specificity and activation of phytochelatin synthases from model plants by physiologically relevant metals. Plant Physiol. 140, 1213–1221. http://dx.doi.org/10.1104/pp.105.073635.

Lütz-Meindl, U., 2016. *Micrasterias* as a model system in plant cell biology. Front. Plant Sci. 7, 1019–1999. http://dx.doi.org/10.3389/fpls.2016.00999.

Marschner, P., 2012. Marschner's Mineral Nutrition of Higher Plants, third ed. Academic Press, Cambridge, MA.

Matsumoto, S., Vestergaard, M., Konishi, T., Nishikori, S., Shiraki, K., Tsuji, N., Hirata, K., Takagi, M., 2009. Role of C-terminal cys-rich region of phytochelatin synthase in tolerance to cadmium ion toxicity. J. Plant Biochem. Biotechnol. 18, 175. http://dx.doi.org/10.1007/BF03263316.

McCourt, R.M., Delwiche, C.F., Karol, K.G., 2004. Charophyte algae and land plant origins. Trends Ecol. Evol. 19, 661–666. http://dx.doi.org/10.1016/j.tree.2004.09.013.

Morris, J.L., Puttick, M.N., Clark, J.W., Edwards, D., Kenrick, P., Pressel, S., Wellman, C.H., Yang, Z., Schneider, H., Donoghue, P.C.J., 2018. The timescale of early land plant evolution. Proc. Natl. Acad. Sci. U. S. A 1–10. https://doi.org/10.1073/pnas.1719588115.

Muneer, S., ByoungRyong, J., Tae-Hwan, K., Jeong Jun, L., Soundararajan, P., 2014. Transcriptional and physiological changes in relation to Fe uptake under conditions of Fe-deficiency and Cd-toxicity in roots of *Vigna radiata* L. J. Plant Res. 127, 731–742. http://dx.doi.org/10.1007/s10265-014-0660-0.

Nakakoshi, M., Nishioka, H., Katayama, E., 2011. New versatile staining reagents for biological transmission electron microscopy that substitute for uranyl acetate. J. Electron. Microsc. 60, 401–407. http://dx.doi.org/10.1093/jmicro/dfr084.

Olsson, S., Penacho, V., Puente-Sánchez, F., Díaz, S., Gonzalez-Pastor, J.E., Aguilera, A., 2017. Horizontal gene transfer of phytochelatin synthases from bacteria to extremophilic green algae. Microb. Ecol. 73, 50–60. http://dx.doi.org/10.1007/s00248-016-0848-z.

Petraglia, A., De Benedictis, M., Degola, F., Pastore, G., Calcagno, M., Ruotolo, R., Mengoni, A., Sanità di Toppi, L., 2014. The capability to synthesize phytochelatins and the presence of constitutive functional phytochelatin synthases are ancestral (plesiomorphic) characters for basal land plants. J. Exp. Bot. 65, 1153–1163. http://dx.doi.org/10.1093/jxb/ert472.

Peng, J.-S., Gong, J.-M., 2014. Vacuolar sequestration capacity and long-distance metal transport in plants. Front. Plant Sci. 19, 23. http://dx.doi.org/10.3389/fpls.2014.00019.

Qiu, Y.L., Li, L., Wang, B., Chen, Z., Knoop, V., Groth-Malonek, M., Dombrovska, O., Lee, J., Kent, L., Rest, J., Estabrook, G.F., Hendry, T.A., Taylor, D.W., Testa, C.M., Ambros, M., Crandall-Stotler, B., Duff, R.J., Stech, M., Frey, W., Quandt, D., Davis, C.C., 2006. The deepest divergences in land plants inferred from phylogenomic evidence. Proc.

Natl. Acad. Sci. U. S. A 103, 15511–15516. http://dx.doi.org/10.1073/pnas.0603335103.
Qiu, Y.L., 2008. Phylogeny and evolution of charophytic algae and land plants. J. Syst. Evol. 46, 287–306. https://doi.org/10.3724/SP.J.1002.2008.08035.
Ramos, J., Naya, L., Gay, M., Abián, J., Becana, M., 2008. Functional characterization of an unusual phytochelatin synthase, LjPCS3, of *Lotus japonicus*. Plant Physiol. 148, 536–545. http://dx.doi.org/10.1104/pp.108.121715.
Rascio, N., Navari-Izzo, F., 2011. Heavy metal hyperaccumulating plants: how and why do they do it? And what makes them so interesting? Plant Sci. 180, 169–181. http://dx.doi.org/10.1016/j.plantsci.2010.08.016.
Rea, P.A., 2012. Phytochelatin synthase: of a protease a peptide polymerase made. Physiol. Plant 145, 154–164. http://dx.doi.org/10.1111/j.1399-3054.2012.01571.x.
Rea, P.A., Vatamaniuk, O.K., Rigden, D.J., 2004. Weeds, worms and more. Papain's long-lost cousin, phytochelatin synthase. Plant Physiol. 136, 2463–2474. http://dx.doi.org/10.1104/pp.104.048579.
Romanyuk, N.D., Rigden, D.J., Vatamaniuk, O.K., Lang, A., Cahoon, R.E., Jez, J.M., Rea, P.A., 2006. Mutagenic definition of a papain-like catalytic triad, sufficiency of the N-terminal domain for single-site core catalytic enzyme acylation, and C-terminal domain for augmentative metal activation of a eukaryotic phytochelatin synthase. Plant Physiol. 141, 858–869. http://dx.doi.org/10.1104/pp.106.082131.
Ruotolo, R., Peracchi, A., Bolchi, A., Infusini, G., Amoresano, A., Ottonello, S., 2004. Domain organization of phytochelatin synthase. Functional properties of truncated enzyme species identified by limited proteolysis. J. Biol. Chem. 279, 14686–14693. http://dx.doi.org/10.1074/jbc.M314325200.
Schneider, S.C., Garcia, A., Martin-Closas, C., Chivas, A.R., 2015. The role of charophytes (Charales) in past and present environments: an overview. Aquat. Bot. 120, 2–6. http://dx.doi.org/10.1016/j.aquabot.2014.10.001.
Tennstedt, P., Peisker, D., Böttcher, C., Trampczynska, A., Clemens, S., 2009. Phytochelatin synthesis is essential for the detoxification of excess zinc and contributes significantly to the accumulation of zinc. Plant Physiol. 149, 938–948. http://dx.doi.org/10.1104/pp.108.127472.
Thompson, A.R., Vierstra, R.D., 2005. Autophagic recycling: lessons from yeast help define the process in plants. Curr. Op. Plant Biol. 8, 165–173. http://dx.doi.org/10.1016/j.pbi.2005.01.013.
Urbaniak, J., Gąbka, M., 2014. Polish Charophytes. An Illustrated Guide to Identification. Uniwersytet Przyrodniczy we Wrocławiu, Wrocław.
Vatamaniuk, O.K., Mari, S., Lu, Y.P., Rea, P.A., 2000. Mechanism of heavy metal ion activation of phytochelatin (PC) synthase. J. Biol. Chem. 275, 31451–31459. http://dx.doi.org/10.1074/jbc.M002997200.
Vivares, D., Arnoux, P., Pignol, D., 2005. A papain-like enzyme at work: native and acyl-enzyme intermediate structures in phytochelatin synthesis. Proc. Natl. Acad. Sci. U. S. A 102, 18848–18853. http://dx.doi.org/10.1073/pnas.0505833102.
Volland, S., Bayer, E., Baumgartner, V., Andosh, A., Lütz, C., Sima, E., Lütz-Meindl, U., 2014. Rescue of heavy metal effects on cell physiology of the algal model system *Micrasterias* by divalent ions. J. Plant Physiol. 171, 154–163. http://dx.doi.org/10.1016/j.jplph.2013.10.002.
Volland, S., Schaumlöffel, D., Dobritzsch, D., Krauss, G.J., Lütz-Meindl, U., 2013. Identification of phytochelatins in the cadmium-stressed conjugating green alga *Micrasterias denticulata*. Chemosphere 91, 448–454. http://dx.doi.org/10.1016/j.chemosphere.2012.11.064.
Vurro, E., Ruotolo, R., Ottonello, S., Elviri, L., Maffini, M., Falasca, G., Zanella, L., Altamura, M., Sanità di Toppi, L., 2011. Phytochelatins govern zinc/copper homeostasis and cadmium detoxification in *Cuscuta campestris* parasitizing *Daucus carota*. Environ. Exp. Bot. 72, 26–33. http://dx.doi.org/10.1016/j.envexpbot.2010.04.017.
Wang, H.C., Wu, J.S., Chia, J.C., Yang, C.C., Wu, Y.J., Juang, R.H., 2009. Phytochelatin synthase is regulated by protein phosphorylation at a threonine residue near its catalytic site. J. Agric. Food Chem. 57, 7348–7355. http://dx.doi.org/10.1021/jf9020152.
Wickett, N.J., et al., 2014. Phylotranscriptomic analysis of the origin and early diversification of land plants. Proc. Natl. Acad. Sci. U. S. A 11, E4859–E4868. http://dx.doi.org/10.1073/pnas.1323926111.
Wodniok, S., Brinkmann, H., Glöckner, G., Heidel, A.J., Philippe, H., Melkonian, M., Becker, B., 2011. Origin of land plants: do conjugating green algae hold the key? BMC Evol. Biol. 11, 104. http://dx.doi.org/10.1186/1471-2148-11-104.
Wojas, S., Clemens, S., Hennig, J., Skłodowska, A., Kopera, E., Schat, H., Bal, W., Antosiewicz, D.M., 2008. Overexpression of phytochelatin synthase in tobacco: distinctive effects of AtPCS1 and CePCS genes on plant response to cadmium. J. Exp. Bot. 59, 2205–2219. http://dx.doi.org/10.1093/jxb/ern092.